Journal of Power Sources, 35 (1991) 163–173

Effect of counter cations on electrocatalytic activity of oxide pyrochlores towards oxygen reduction/evolution in alkaline medium: an electrochemical and spectroscopic study

A. K. Shukla, A. M. Kannan, M. S. Hegde and **J. Gopalakrishnan**
Solid State and Structural Chemistry Unit, Indian Institute of Science, Bangalore-560 012 (India)

(Received December 13, 1990)

Abstract

A systematic electrochemical and spectroscopic study is conducted to examine the effect of counter cations on the electrocatalytic activities of oxide pyrochlores towards oxygen reduction and evolution reactions in alkaline medium. The study suggests that among the family of oxide pyrochlores, $Pb_2Ir_2O_{7-y}$ and $PbBiRu_2O_{7-y}$ are efficient and stable bifunctional oxygen catalysts. An analysis of the X-ray photoelectron spectra of the oxide pyrochlores supports the postulated pathways for the oxygen reactions.

Introduction

The development of a stable and cost-effective air electrode for a secondary metal/air cell is a challenging technical target. Only a few catalytic materials are known to both reduce and evolve oxygen effectively under the relatively unforcing conditions required to make metal/air cells economically attractive.

In recent years, metal oxides have been investigated as possible bi-directional catalysts for both the oxygen-evolution reaction (OER) and the oxygen-reduction reaction (ORR) [1–5]. The defect pyrochlores $A_2B_2O_6O'_{1-y}\square_y$ ($0 \leqslant y \leqslant 1$) with A = Pb and/or Bi and B = Ru or Ir represent a family of oxides that has been found to function bi-directionally [6–11]. These materials are therefore particularly useful for conducting fundamental studies of the reaction pathways of both the OER and the ORR.

The pyrochlore structure consists of a B_2O_6 framework of corner-shared (BO_6) octahedra with a bent ($\times 135°$) B–O–B bond angle. In the family of interest, the B_2O_6 framework is metallic. The larger A cations, which may be considered the 'counter cations', reside with the O′-oxygen coordinated by two A and two B cations. Each A cation of an ideal pyrochlore is coordinated by six O-atoms of a flattened octahedron and two O′-oxygens that cap the two large faces of the flattened octahedron. If the larger A cations retain

0378-7753/91/$3.50

$6s^2$ cores, as is the case for Tl^+, Pb^{2+}, and Bi^{3+} ions, the pyrochlore structure commonly contains O′-oxygen vacancies, □ [12].

Goodenough *et al.* [13, 14] have used measurements of the surface charge of colloidal particle versus solution pH in conjunction with electrochemistry to conclude that the OER occurs at the O-oxygen atoms because the equilibrium reaction

$$B^{5+}–O^{2-} \rightleftharpoons B^{4+}–O^{-} \quad (1)$$

at the surface is not biased strongly to the left, whereas the ORR occurs via an outer-sphere reaction followed by an exchange reaction at an O′ site, i.e.,

$$O_2 + e^- \longrightarrow O_2^- \quad (2)$$

$$A\text{-}OH^- + O_2^- \longrightarrow AO_2^- + OH^- \quad (3)$$

in alkaline solution. Either reaction (2) or (3) could be rate limiting; in the cases studied it was reaction (3). A change of mechanism for the ORR was correlated with the solution pH at zero applied potential below which the equilibrium

$$A\text{-}OH^- + H^+ \rightleftharpoons A\text{-}OH_2 \quad (4)$$

becomes biased strongly to the right. This correlation is considered appropriate because the principal surface changes accompanying the application of an applied voltage should occur in the metallic B_2O_6 framework.

With such a model for the reaction pathways, it is then natural to ask how these reactions are modified by a change of counter cation and whether these modifications can be rationalized on the basis of the proposed models. In this study, these questions are addressed by the use of X-ray photoelectron and absorption near-edge spectroscopies in conjunction with electrochemistry.

Experimental

Preparation of oxide catalysts

Several oxide pyrochlores containing Pb or Ag (Table 1) were prepared by heating a mixture of the respective oxides in air at 1073 K for 12 h. $Bi_2Ru_2O_7$ and its Tl-substituted solid solutions were prepared similarly, but fired in an evacuated, sealed quartz tube. The formation of single-phase oxide pyrochlores was confirmed by powder X-ray diffraction analysis with a JEOL JDX-8P powder X-ray diffractometer.

A Pt-black sample was prepared by reduction of an aqueous solution of H_2PtCl_6 with 5 wt.% sodium formate solution [15].

Preparation of electrodes

The electrode substrate comprising the oxide pyrochlore suspended in cyclohexane and an optimum quantity (16 wt.%) of Fluon-GP2 PTFE suspension, was mixed by agitating in an ultrasonic bath. The resulting mass

TABLE 1

Oxygen reduction (ORR) and oxygen evolution (OER) currents as obtained from the respective cyclic voltammograms of various pyrochlore oxide-based electrodes

Oxide catalyst	Reduction current at −200 mV (mA cm^{-2})	Oxidation current at +650 mV (mA cm^{-2})
$Pb_2Ir_2O_{7-y}$	130	113
$Pb_2Ru_2O_{7-y}$	Unstable	133
$Pb_{1.5}Bi_{0.5}Ru_2O_{7-y}$	87	103
$PbBiRu_2O_{7-y}$	107	170
$Bi_{1.5}Pb_{0.5}Ru_2O_{7-y}$	55	173
$Bi_2Ru_2O_7$	67	207
$Bi_{1.5}Tl_{0.5}Ru_2O_{7-y}$	100	60
$Bi_{1.5}Ag_{0.5}Ru_2O_{7-y}$	60	250
Pt-black	220	92

was dried in an air oven at 100 °C and the electrodes were prepared by cold compacting the hydrophobized oxide between two nickel screens (~2200 mesh cm^{-2}) under a hydraulic press at an optimum pressure of 180 kg cm^{-2} for 225 s [4]. Under these conditions, circular electrodes (area 2.5 cm^2, thickness 0.1 cm) were prepared for cyclic voltammetric and galvanostatic polarization studies. In this configuration, the nickel screen placed on the rear side of the electrode substrate, i.e., the gas side, acts as the current collector while the other facing the electrolyte provides the site for the oxygen evolution reaction [8].

Electrochemical characterization of electrodes

Several repetitive cyclic voltammograms (CV) were obtained for the pyrochlore-based electrodes in 6 M KOH solution at 30 °C. These were recorded using a PAR Model 173 Potentiostat/Galvanostat coupled to a Model 175 Universal Programmer in the potential range −200 to +650 mV versus a pre-calibrated Hg/HgO, OH^- (6 M KOH) reference electrode. All potentials are reported with regard to the latter electrode.

The electrodes were also subjected to repeated steady-state galvanostatic polarization at 30 °C for both the OER and the ORR with a three-electrode cell having a sintered-nickel counter electrode and an Hg/HgO, OH^- (6 M KOH) reference electrode [4]. Oxygen gas at a pressure of 30 mmHg was fed from the rear of the oxide-based electrode during the ORR experiment.

Physicochemical characterization of oxide catalysts

X-ray-absorption near-edge spectroscopy (XANES) and photoelectron spectroscopy (PES) were carried out on powdered specimens. Samples for XANES consisted of a fine powder of the oxide catalyst sandwiched between two adhesive tapes. Room temperature Pb (L_{III}) and Bi (L_{III}) spectra were recorded with a Rigaku X-ray absorption spectrometer coupled to an Ru-200 B Rigaku rotating anode X-ray generator. The monochromator was an

Si (440) crystal with a 0.1 mm slit. Spectra were recorded in 0.1 eV steps in the regions of interest.

X-ray and UV PES studies were made with an ESCA LAB-5 system and Al Kα X-ray photons or He-II UV radiation, respectively. None of these metallic samples exhibited any charging. The Pb(4f), Bi(4f), Ru(3d), and O(1s) core levels and the valence band were examined. The reported binding energies are with reference to the Au($4f_{7/2}$) level at 83.7 eV and are accurate to within ± 0.02 eV. The absence of a C(1s) peak at 289 eV showed that none of the samples was contaminated with CO_3^{2-}; even the graphitic-carbon impurity concentration was low (surface concentration < 0.17).

Results and discussion

The CV data for the oxide pyrochlores listed in Table 1 are compared in Fig. 1 with the CV for a Pt-black electrode. With the exception of $Pb_2Ru_2O_{7-y}$, all the oxides were stable (i.e., showed no variation in the CV on repeated cycling) towards the ORR and OER in the alkaline solution. The reduction and oxidation currents at specified potentials are given in Table 1. From these data, it can be seen that the optimum bi-directional activity was exhibited by the $Pb_2Ir_2O_{7-y}$ and $PbBiRu_2O_{7-y}$ oxide-based electrodes.

Polarization curves for the Ru-pyrochlore electrodes are compared in Fig. 2; Tafel slopes and exchange-current densities are given in Table 2.

The X-ray PES Ir(4f) spectra for elemental Ir, IrO_2, and $Pb_2Ir_2O_{7-y}$ are presented in Fig. 3. Whereas metallic Ir exhibits binding energies of 61.2 eV ($4f_{7/2}$) and 64.2 eV ($4f_{5/2}$), both IrO_2 and $Pb_2Ir_2O_{7-y}$ give binding energies of 62.6 eV ($4f_{7/2}$) and 65.6 eV ($4f_{5/2}$) corresponding to a 1.4 eV core-level shift. These observations indicate that, in zero-applied field, the valence state of the near-surface iridium in $Pb_2Ir_2O_{7-y}$ is Ir^{4+}, which is consistent with

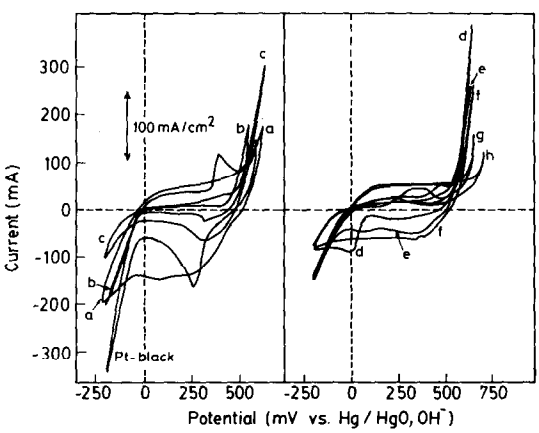

Fig. 1. Cyclic voltammograms for oxygen electrodes containing: (a) $Pb_2Ir_2O_{7-y}$; (b) $Pb_2Ru_2O_{7-y}$; (c) $Bi_2Ru_2O_7$; (d) $Bi_{1.5}Ag_{0.5}Ru_2O_{7-y}$; (e) $PbBiRu_2O_{7-y}$; (f) $Bi_{1.5}Pb_{0.5}Ru_2O_{7-y}$; (g) $Pb_{1.5}Bi_{0.5}Ru_2O_{7-y}$; (h) $Bi_{1.5}Tl_{0.5}Ru_2O_{7-y}$. 6 M KOH at 30 °C; scan rate: 5 mV s^{-1}.

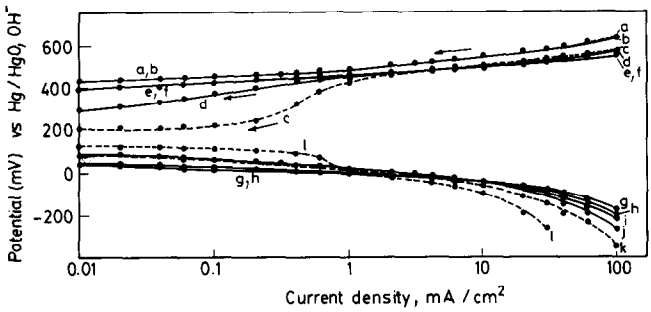

Fig. 2. Galvanostatic polarization curves towards OER and ORR (without iR-compensation) in 6 M KOH at 30 °C for oxygen electrodes containing: (a), (k) $Bi_{1.5}Pb_{0.5}Ru_2O_{7-y}$; (b), (i) $Bi_{1.5}Tl_{0.5}Ru_2O_{7-y}$; (c), (l) $Bi_{1.5}Ag_{0.5}Ru_2O_{7-y}$; (d), (j) $Bi_2Ru_2O_7$; (e), (g) $PbBiRu_2O_{7-y}$; (f), (h) $Pb_{1.5}Bi_{0.5}O_{7-y}$.

TABLE 2

Kinetic parameters from galvanostatic polarization plots for various pyrochlore oxide-based electrodes towards oxygen reduction (ORR) and oxygen evolution (OER)

Oxide catalyst	Tafel slope (mV/decade)		Exchange current density (mA cm^{-2})	
	ORR	OER	ORR $\times 10^{-4}$	OER $\times 10^{-4}$
$Pb_2Ir_2O_{7-y}$	55	30	1.5	0.01
$Pb_2Ru_2O_{7-y}$	–	35	–	4
$Pb_{1.5}Bi_{0.5}Ru_2O_{7-y}$	50	40	0.2	2
$PbBiRu_2O_{7-y}$	45	35	0.02	1
$Bi_{1.5}Pb_{0.5}Ru_2O_{7-y}$	80	55	0.9	3
$Bi_2Ru_2O_7$	55	45	0.025	2
$Bi_{1.5}Tl_{0.5}Ru_2O_{7-y}$	60	55	0.6	3
$Bi_{1.5}Ag_{0.5}Ru_2O_{7-y}$	–	45	–	2

a measured bulk value $y = 0.9$ [15]. With only 0.1 O′-oxygen per formula unit, the surface is expected to be completely stripped of O′ atoms, and, indeed, the measurement of surface charge versus solution pH of colloidal $Pb_2Ir_2O_{7-y}$ also indicated a complete absence of O′-oxygen in the dry state [13]. The accuracy of the XPS measurements here is not, however, sufficient to distinguish between a valence of 4.1+ and 4+.

The X-ray PES Ru(3d) core-level spectra for RuO_2, $Bi_2Ru_2O_7$, $BiPbRu_2O_{7-y}$ and $Pb_2Ru_2O_{7-y}$ are given in Fig. 4. All the oxides are metallic and there is no apparent shift of the binding energies in any of these samples from their positions in RuO_2, where Ru is formally Ru^{4+}. With $y = 0.5$ in $Pb_2Ru_2O_{7-y}$ this finding would again suggest that the surface is depleted of O′ ions under the high-vacuum conditions of the experiment. By contrast, measurements of surface charge versus solution pH of colloidal $Pb_2Ru_2O_{7-y}$ clearly

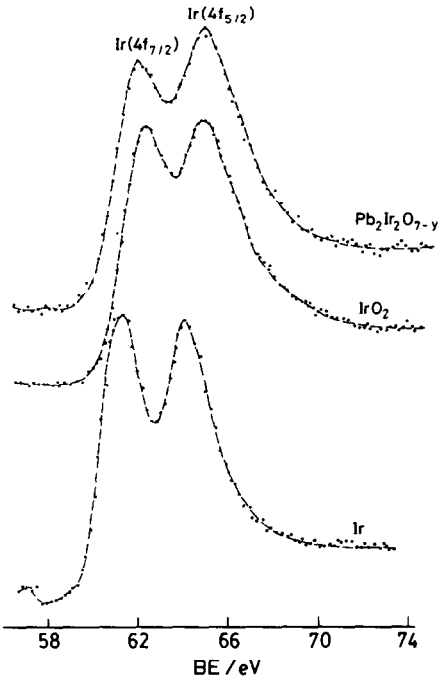

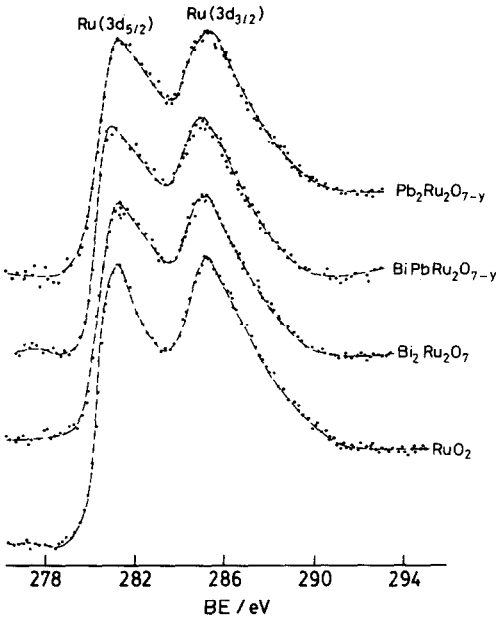

Fig. 3. X-ray photoelectron core level spectra of Ir(4f) for Ir, IrO_2, and $Pb_2Ir_2O_{7-y}$.

Fig. 4. X-ray photoelectron core level spectra of Ru(3d) for RuO_2, $Bi_2Ru_2O_7$, $BiPbRu_2O_{7-y}$, and $Pb_2Ru_2O_{7-y}$.

demonstrated the presence of surface O′-oxygen in samples not subjected to a vacuum [13].

XANES has been shown [17–19] to be a sensitive technique for detecting the oxidation states of cations in oxides. The Bi(L_{III}) and Pb(L_{III}) XANES spectra for elemental Bi and PbO are compared in Fig. 5 with those for Bi_2O_3, PbO_2, and the pyrochlores. The data indicate that the Bi and Pb atoms in the pyrochlores have the formal valence states Bi^{3+} and Pb^{2+}. Moreover, the Pb(4f) and Bi(4f) X-ray PES core-level spectra for $Bi_2Ru_2O_7$ and $BiPbRu_2O_{7-y}$ (Fig. 6) exhibit binding energies of: (i) 138 eV ($4f_{7/2}$) and 142.8 eV ($4f_{5/2}$), similar to those reported for Pb^{2+} [19]; (ii) 158.3 eV ($4f_{7/2}$) and 163.7 eV ($4f_{5/2}$), similar to those for Bi^{3+} [20]. Horowitz *et al.* [21] have also indicated that lead-containing pyrochlores synthesized by a high-temperature route always lead to compounds with Pb in the Pb^{2+} valence state.

Of more interest are the O(1s) core-level spectra. Data given in Fig. 7 reveal a shift in the binding energy from 530 eV in IrO_2 to 529 eV in $Pb_2Ir_2O_{7-y}$. A higher binding energy indicates a smaller screening of the O(1s) electron from the nuclear charge by the outer electrons and, hence, a greater transfer of the outer O=2s, 2p electrons from the oxygen back to the neighboring cations. Whereas each of the oxygen atoms of IrO_2 have three Ir^{4+} near neighbours, the O′-oxygens of $Pb_2Ir_2O_{7-y}$ have two Ir^{4+} and

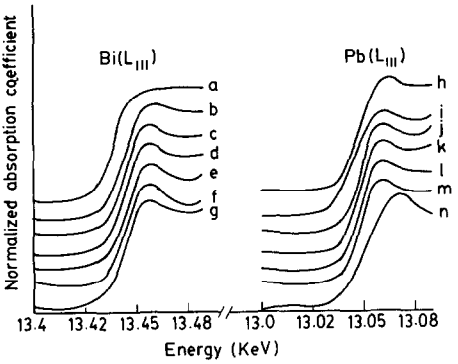

Fig. 5. Normalized Bi(L_{III}) XANES of: (a) Bi metal; (b) Bi_2O_3; (c) $Bi_2Ru_2O_7$; (d) $Bi_{1.5}Pb_{0.5}Ru_2O_{7-y}$; (e) $BiPbRu_2O_{7-y}$; (f) $Bi_{0.5}Pb_{1.5}Ru_2O_{7-y}$; (g) $Bi_{1.5}Tl_{0.5}Ru_2O_{7-y}$. Normalized Pb($L_{III}$) XANES of: (h) PbO; (i) $Pb_2Ir_2O_{7-y}$; (j) $Pb_2Ru_2O_{7-y}$; (k) $Pb_{1.5}Bi_{0.5}Ru_2O_{7-y}$; (l) $PbBiRu_2O_{7-y}$; (m) $Pb_{0.5}Bi_{1.5}Ru_2O_{7-y}$; (n) PbO_2.

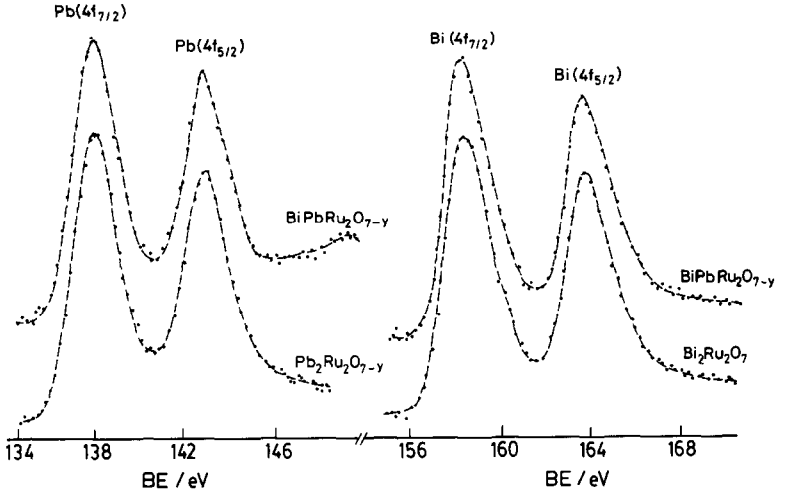

Fig. 6. X-ray photoelectron core level spectra of Pb(4f) for $Pb_2Ru_2O_{7-y}$ and $PbBiRu_2O_{7-y}$, and of Bi(4f) for $Bi_2Ru_2O_7$ and $BiPbRu_2O_{7-y}$.

two Pb^{2+} ions. The data of Fig. 7 show that there is more back transfer of electronic charge from the oxide ions to one Ir^{4+} than there is to two Pb^{2+} ions.

The O(1s) spectra for several ruthenium compounds are displayed in Fig. 8. A similar shift from 530 eV in RuO_2 to about 529 eV in $Pb_2Ru_2O_{7-y}$ is found. The shift from 530 eV is smaller in $Bi_2Ru_2O_7$; but it is still negative, which suggests that there is less electron transfer from the O-oxygen to two Bi^{3+} ions than to two Pb^{2+} ions, as must be expected.

The valence-band spectra of IrO_2 and $Pb_2Ir_2O_{7-y}$ are compared in Fig. 9. The spectrum of IrO_2 has an Ir-5d band at the Fermi energy, E_F, overlapping a broad O-2p band. The features of this spectrum agree well with those

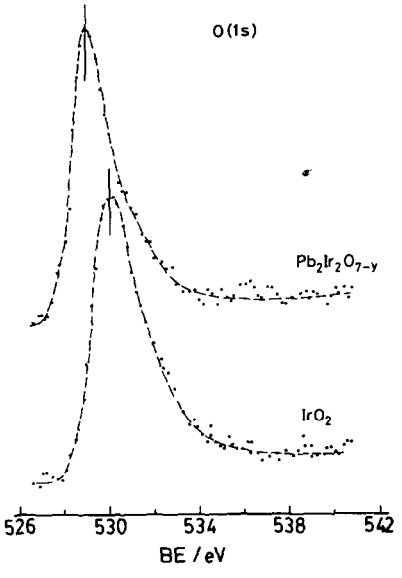

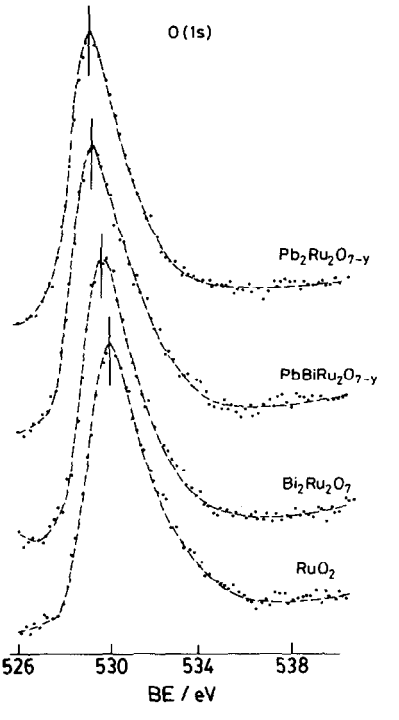

Fig. 7. Core level O(1s) spectra of IrO_2 and $Pb_2Ir_2O_{7-y}$.

Fig. 8. Core level O(1s) spectra of RuO_2, $Bi_2Ru_2O_7$, $PbBiRu_2O_{7-y}$, and $Pb_2Ru_2O_{7-y}$.

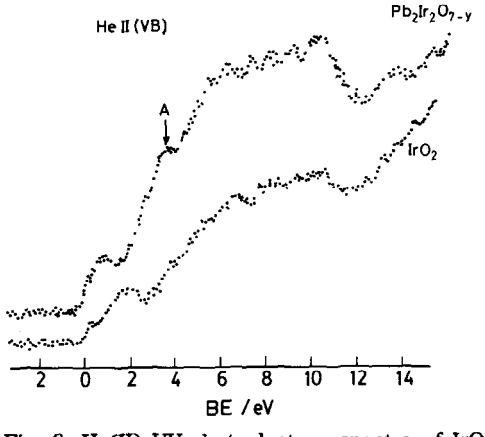

Fig. 9. He(II) UV photoelectron spectra of IrO_2 and $Pb_2Ir_2O_{7-y}$.

previously reported [22]. The spectrum of $Pb_2Ir_2O_{7-y}$ is similar, but it exhibits a distinct new band, marked A, emerging near 3 eV below E_F. The spectra of the ruthenium-based pyrochlores and RuO_2 are given in Fig. 10. A similar peak, A, emerges in all the pyrochlore spectra about 4 eV below E_F. It is

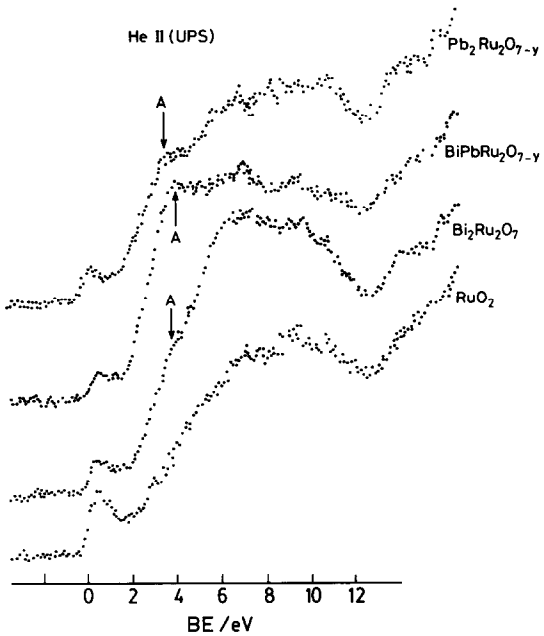

Fig. 10. He(II) UV photoelectron spectra of RuO_2, $Bi_2Ru_2O_7$, $BiPbRu_2O_{7-y}$, and $Pb_2Ru_2O_{7-y}$.

not specific to Pb^{2+}, but it may be somewhat more pronounced in $Pb_2Ru_2O_{7-y}$ than in $Bi_2Ru_2O_7$. Since the O-2p electrons have a higher cross-section for photoionization with He-II radiation [22], band A is taken to be an O-2p band that is raised in energy relative to the other O-2p states. It does not appear to be due to the O'-oxygen, since few of these appear to be present near the surface, particularly in the case of $Pb_2Ir_2O_{7-y}$. The fact that there is no significant shift on going from $Bi_2Ru_2O_7$ to $Pb_2Ru_2O_{7-y}$ would appear to rule out a direct excitation of $6s^2$ core electrons. Therefore, it must be concluded that peak A originates from O-2p states with energies that have been raised by hybridization with lower-lying $6s^2$ core electrons on the A cations. Since the $6s^2$ core electrons of Bi^{3+} ions lie deeper in energy than those of Pb^{2+} ions, the O-2p hybridization with A-6s electrons may be stronger for Pb^{2+} than for Bi^{3+} ions.

An important point is that the valence-band spectra of Figs. 9 and 10 demonstrate that the top of the O-2p band is within 2 eV of the Fermi energy in the Ru-4d or Ir-5d bands of the Ru(IV) and Ir(IV) oxides. A correlation splitting of 1–2 eV for the narrow d bands would clearly make the equilibrium of eqn. (1) nearly balanced without any strong bias to the left. Thus, the criterion for a facile OER developed previously [13, 14] is shown to be satisfied.

The fact that the rare-earth pyrochlores $Ln_2Ru_2O_7$ are anti-ferromagnetic semiconductors [24] suggests that the correlation energy (U) of the Ru-4d electrons cannot be neglected. On the other hand, the $Pb_2Ru_2O_{7-y}$ and

$Bi_2Ru_2O_7$ pyrochlores are metallic as a result of interactions between the A cations and the Ru-4d bands [25]. This fact raised the question as to whether the broadening of the Ru-4d or Ir-5d bands is due primarily to an interaction between either the occupied d states and the empty A-cation 6p states, or the empty d states and the occupied A-cation 6s states. Whereas Goodenough and co-workers [16, 26, 27] originally assumed the latter was dominant on the basis of the known stability of Pb(IV) and Bi(V) species in octahedral coordination, Hsu *et al.* [28] carried out self-consistent calculations that indicated a Pb-$6s^2$ core some 8 eV below E_F in $Pb_2Ru_2O_{7-y}$, but a Pb-6p band only 1–2 eV above E_F. These authors have therefore argued that the empty A-cation 6p states are primarily hybridizing with the B-cation d bands to broaden them.

In support of Hsu *et al.* [28], our interpretation of peak A in the valence band spectra of the pyrochlores requires placement of the $6s^2$ core levels at least 5 eV below E_F, and perhaps as much as 8 eV. Given this fact, it is extremely interesting to observe how sensitive the position of a given outer-electron energy level is to the metal–oxygen coordination and bond length since, in these same pyrochlores, stabilization of Pb^{4+} and Bi^{5+} in the octahedral sites is found, particularly with low temperature preparations [29]. A shift of 10 eV in the energy of the $6s^2$ core energies is required on going from the A to the B sites; such an extreme sensitivity would well account for the observation of the 'negative U' disproportionation reactions:

$$2Pb^{3+} \longrightarrow Pb^{2+} + Pb^{4+} \quad (5)$$

$$2Bi^{4+} \longrightarrow Bi^{3+} + Bi^{5+} \quad (6)$$

On the other hand, the appearance of peak A suggests that the O-2p interactions with the A-cation $6s^2$ core levels is important and therefore could give rise to significant B–O–A interactions between the B-cation d states and the A-cation 6s electrons. Moreover, a reduced binding energy for the O(1s) core level in the pyrochlores relative to the rutile phases RuO_2 and IrO_2 suggests that hybridization of the O-2p and A-cation 6p states may not be as strong as the calculations of Hsu *et al.* [28] would imply.

Acknowledgements

The authors are indebted to Professor S. Sathyanarayana and Professor C. N. R. Rao for their kind encouragement, and to Dr G. Sankar for assistance in obtaining XANES data. Thanks are also due to Professor J. B. Goodenough for valuable comments. AKS is grateful to the Department of Non-Conventional Energy Sources, Government of India, New Delhi, for supporting this research. AMK thanks the Council of Scientific and Industrial Research, New Delhi, for a Senior Research Fellowship.

References

1 S. Viswanathan and A. Charkey, *SAE Tech. Pap. No. 859053*, 1985, p. 2.21.
2 A. M. Trunov, A. I. Kotseruba, N. M. Yakovleva and V. E. Polishchuk, *Elektrokhimiya, 14* (1978) 1165.
3 L. Swette and J. Giner, *J. Power Sources, 22* (1988) 399.
4 A. M. Kannan, A. K. Shukla and S. Sathyanarayana, *J. Power Sources, 25* (1989) 141.
5 W. L. Fielder and J. Singer, in R. E. White and A. J. Appleby (eds.), *Proc. Symp. Fuel Cells, California, Nov. 6–7, 1989*, The Electrochem. Soc., Inc., NJ, 1989, p. 291.
6 H. S. Horowitz, J. M. Longo and J. I. Haberman, *U.S. Patent 4 146 458* (1979).
7 H. S. Horowitz, J. M. Longo and H. H. Horowitz, *J. Electrochem. Soc., 130* (1983) 1851.
8 A. M. Kannan, A. K. Shukla and S. Sathyanarayana, *J. Electroanal. Chem., 281* (1990) 339.
9 J. A. R. Van Veen, J. M. Van Der Eijk, R. De Ruiter and S. Huizinga, *Electrochim. Acta, 33* (1988) 51.
10 J. Prakash, D. Tryk and E. Yeager, *J. Power Sources, 29* (1990) 413.
11 A. M. Kannan and A. K. Shukla, *J. Power Sources, 35* (1991) 00.
12 M. A. Subramanian, G. Aravamudan and G. V. Subba Rao, *Prog. Solid State Chem., 15* (1983) 71.
13 J. B. Goodenough, R. Manoharan and M. Paranthaman, *J. Am. Chem. Soc., 112* (1990) 2076.
14 R. Manoharan, M. Paranthaman and J. B. Goodenough, *Eur. J. Solid State Inorg. Chem., 26* (1989) 155.
15 K. V. Ramesh, P. R. Sarode, S. Vasudevan and A. K. Shukla, *J. Electroanal. Chem., 223* (1987) 91.
16 J. M. Longo, P. M. Raccah and J. B. Goodenough, *Mater. Res. Bull., 4* (1969) 191.
17 J. B. Parise, P. L. Gai, M. A. Subramanian, J. Gopalakrishnan and A. W. Sleight, *Physica, C159* (1989) 245.
18 G. U. Kulkarni, G. Sankar and C. N. R. Rao, *Appl. Phys. Lett., 55* (1989) 388.
19 V. Vijayakrishnan, G. U. Kulkarni and C. N. R. Rao, *Mod. Phys. Lett., B4* (1990) 451.
20 M. S. Hegde and P. Ganguly, *Phys. Rev. B, 38* (1988) 4557; P. Ganguly and M. S. Hegde, *Phys. Rev. B, 37* (1988) 5107.
21 H. S. Horowitz, J. M. Longo and J. T. Lewandowski, *Mater. Res. Bull., 16* (1981) 489.
22 J. H. Xu, T. Jarlborg and A. J. Freeman, *Phys. Rev. B, 40* (1989) 7939.
23 C. S. Fadley, *J. Electron Spectrosc. Relat. Phenom., 21* (1981) 285.
24 J. B. Goodenough, A. Hamnett and D. Telles, in H. Fritzsche and D. Adler (eds.), *Localization and Metal–Insulator Transitions*, Plenum, New York, 1985, p. 161.
25 R. G. Egdell, J. B. Goodenough, A. Hamnett and C. C. Naish, *J. Chem. Soc., Faraday Trans. 1, 79* (1983) 893.
26 P. A. Cox, R. G. Egdell, J. B. Goodenough, A. Hamnett and C. C. Naish, *J. Phys. C, 16* (1983) 6221.
27 P. A. Cox, J. B. Goodenough, P. J. Tavener, D. Telles and R. G. Egdell, *J. Solid State Chem., 62* (1986) 360.
28 W. Y. Hsu, R. V. Kasowski, T. Miller and T. Chiang, *Appl. Phys. Lett., 52* (1988) 792.
29 H. S. Horowitz, J. M. Longo and J. T. Lewandowski, in S. L. Holt (ed.), *Inorganic Synthesis*, Vol. 22, Wiley, New York, 1983, p. 69.